International Journal of Steel Structures
December 2010, Vol 10, No 4, 419-430

International Journal of
STEEL
STRUCTURES
www.ijoss.org

Compressive Behavior of T-shaped Concrete Filled Steel Tubular Columns

Yuanlong Yang, Hua Yang*, and Sumei Zhang

School of Civil Engineering, Harbin Institute of Technology, Harbin, 150090, China

Abstract

Special-shaped column structures improve residential architectural space, compared with traditional frame structures. However, in respect to applicable building height and seismic fortification intensity, traditional special-shaped reinforced concrete (RC) columns have strict limitations in seismic behavior, which hampers further generalization and application of special-shaped columns. Due to increase in constraint effect for concrete, special-shaped concrete-filled steel tube (CFST) columns are expected to behave advantages on the strength, ductility and seismic behavior over special-shaped RC columns. However, special attention should be paid to prevent the steel plates' premature local buckling and the separation between steel tube and concrete at inner corners. The battlement-shaped bar stiffeners and tensile bar stiffeners, welded on tube surfaces, were first put forward in this paper. Experimental study of 9 stubs in three groups subjected to axial loads was conducted, and the specimens consist of 3 square stubs (including 1 non-stiffened and 2 stiffened CFST specimens) and 6 T-shaped stubs (including 1 RC specimen, 2 non-stiffened and 3 stiffened CFST specimens). Failure modes and static properties of the specimens were investigated. Experimental results reveal that: Due to the constraint effect provided by T-shaped tubes, the CFST specimens behave advantages on the RC specimen in the ascending stiffness, peak resistance and ductility (except for the battlement-shaped bar stiffened CFSTs). For square and T-shaped stiffened CFST specimens, the stiffeners improve their ductility, especially the tensile bar which gives the best performance in ductility and improves the peak resistance substantially. The stiffeners postpone the buckling of tubes, and even upgrade the classification of composite sections, without thickening the tubes.

Keywords: T-shape, stiffener, special-shaped column, axial load, constraint effect

1. Introduction

In traditional frame structures, columns normally have larger cross-sectional depths than those of their adjacent walls, with exposed corners to indoor space, which leads to reduction of usable area and disturbance to indoor environment. Recently, special-shaped columns have been increasingly introduced into residential and official buildings, to save indoor efficient room and be conducive to place furniture.

Engineering practices at present is the reinforced concrete (RC) special-shaped column, and some sophisticated achievements have been made by scholars. Previous study focused mainly on the static behavior of T-shaped and L-shaped stub columns, subjected to biaxial eccentric loading, and some correlation curves of resistance were put forward (Joaquin, 1979; Cheng and Hsu, 1989; Mallikarjuna and Mahadevappa, 1992; Dundar and Sahin, 1993; Yau *et al*., 1993). Since the year of 2000, further study carried extensively by Chinese researchers (Zhang and Ye, 2003; Gao *et al*., 2005; Wang *et al*., 2007) has concentrated on the comprehensive static and seismic behavior, especially for members in structural systems, directly for engineering promotions and applications.

However, some problems are revealed from above research: compared with the rectangular column, the cross-section of special-shaped column is spread and its depth is relatively large, and its related high shear deformation percentage causes disadvantages on the resistance and seismic behavior; thin web is prone to be damaged prior to flange, resulting in insufficient material exploration; the frame joint is comparatively weak due to its dimensions, and the shear-resistance of joints cannot fully guarantee bearing applied loads; the resistance is sensitive to horizontal loading direction, and may vary within wide limits when loading direction changes. The disadvantages mentioned above lead to limitations in seismic behavior of RC special-shaped columns: only apply to eight-degree seismic fortification zone (0.2 g) or

Note.-Discussion open until May 1, 2011. This manuscript for this paper was submitted for review and possible publication on July 25, 2010; approved on December 15, 2010

*Corresponding author
Tel: +86-451-8628-2079; Fax: +86-451-8628-2083
E-mail: yanghua@hit.edu.cn

below, and the applicable height of building is subjected to strict restrictions. These limitations are based on the China National code which is focus on the special-shaped columns (JGJ 149-2006/JGJ 514-2006).

To improve its seismic behavior, scholars in China have engaged in research and promotion of special-shaped concrete-filled steel tubes (CFSTs). Axially loaded test research on T-shaped, L-shaped CFST stubs with pulled binding bars (Cai and He, 2005) and ribs (Chen, 2003) were conducted. Mechanism of stiffeners and their improvement on static behavior were focused on and the influencing laws of parameters on sectional resistance were paid attention to. Pseudo-static performance of T-shaped, L-shaped CFST columns under cyclic horizontal loads were studied, and the influencing laws of concrete strength, steel strength and axial load ratio were investigated (Wang and Lv, 2005). To postpone the premature tube buckling and improve the confinement for concrete, reinforcement stiffeners were introduced in pseudo static experiment (Wang *et al*., 2009), and preliminary achievement was made.

Battlement-shaped bar stiffeners and tensile bar stiffeners were first proposed in this paper, to postpone the premature buckling of steel tubes. The mechanism of stiffeners and their enhancement in static behavior of specimens were researched. Experiment of T-shaped CFST stubs subjected to axial load was conducted, along with square CFST stubs for supplementary research on stiffener behavior. Failure modes and static properties of the specimens were investigated, and the experimental conclusions and experience for engineering promotions and applications are provided.

2. Experimental study

2.1. Details of the specimens

Nine stub specimens in three groups were tested, in which two cross sectional shape – square and T-shape, and two kinds of stiffeners – battlement-shaped bar and tensile bar/strip, were considered. The basic geometric properties of the specimens are summarized in Table 1. The SVR is the volumetric ratio of steel (including tube, longitudinal reinforcement, hoop, stiffener, if any) to the specimen, and reveals the steel utilization ratio to promote the behavior of specimens. The investigation focused on the cross-sectional behavior, thus the length to cross-sectional width of all the specimens was around 3:1. This ratio has been proved (Tao *et al*., 2005) to effectively avoid the effect of both overall buckling and end constraint. So the specimen length was determined as 600 mm for Group I and 900 mm for Group II and III. The cross sections of the specimens are listed in Fig. 1.

Two kinds of stiffeners, the battlement-shaped bar and the tensile bar/strip, to restrain the low-order buckling modes, were investigated in the test. The battlement-shaped bar was formed by bending straight hot-rolled plane bar into battlement shape, and then welded on the interior surfaces of the tube. This bar stiffener is expected to restrain the tube at the welds, and the battlement shape guarantees the embedment in concrete. The detailed dimensions are shown in Fig. 2, in which the embedded depth is 50 mm and the spacing L between two welds is 100 mm for Group II and 80 mm for the rest groups.

The tensile bar/strip stiffener employed the straight hot-rolled plane bars/steel plates. Holes with diameters slightly larger than those of the stiffeners were reserved for the stiffeners to pass through. The tensile stiffener was then welded through the holes at two ends, with the longitudinal spacing for the tensile stiffeners being 100 mm. The S-3 specimen employed the tensile strip, with the cross-sectional dimension of 20 mm (height)×3.5 mm (thickness). The gas cutting of strip holes on the tube caused hot-induced initial imperfection, and deteriorated the mechanical property, so the method of hole drilling welded through by tensile plane bar was put forward in the stiffened T-shaped CFST specimens.

During processing of the tube, the steel plates were folded and welded into square or T-shaped cross-sectional hollow tube. For the stiffened specimens, the tubes' welding was after the setting of battlement-shaped bars, but prior to the setting of tensile bars/strips. The cross sections of hollow tubes are shown in Fig. 3. The tubes were welded afterwards with an end plate on the bottom. This fabrication procedure reduced adverse influence

Table 1. Parameters of specimens

Group	Specimen	Cross-section	Stiffener pattern	Concrete strength f_{ck} (MPa)	Tube's yielding strength f_y (MPa)	SVR (%)
I	S-1	Non-stiffened Square CFST	-	37.5	315	7.1
	S-2	Stiffened Square CFST	Battlement-shaped bar	37.5	315	7.9
	S-3	Stiffened Square CFST	Tensile strip	37.5	315	7.7
II	T-1	Non-stiffened T-shaped CFST	-	35.0	162	4.8
	T-2	Stiffened T-shaped CFST	Battlement-shaped bar	35.0	162	5.5
III	T-3	T-shaped RC	-	23.2	-	4.0
	T-4	Non-stiffened T-shaped CFST	-	23.2	315	7.7
	T-5	Stiffened T-shaped CFST	Battlement-shaped bar	23.2	315	8.7
	T-6	Stiffened T-shaped CFST	Tensile bar	23.2	315	8.1

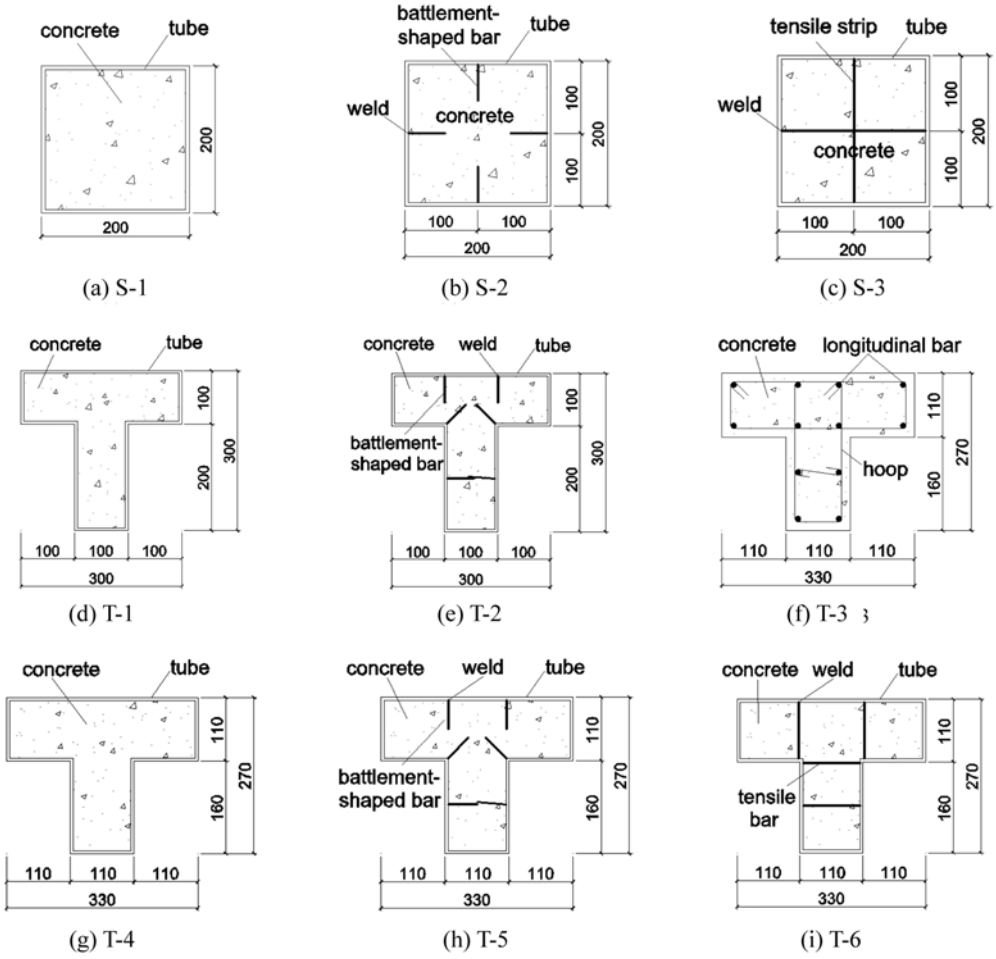

Figure 1. Cross-sectional dimensions of specimens.

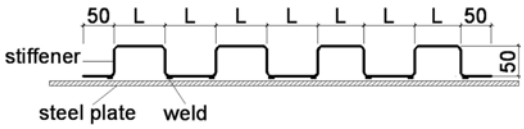

Figure 2. Battlement-shaped bar stiffener.

caused by welding residual stress comparing with traditional treatment. End ribs with the dimensions of 50 mm× 20 mm×3.5 mm were welded at the end of the tubes to reinforce the tubes' end regions.

Layered concrete pouring process was adopted. The hollow tube was put vertically and the concrete was vibrated with an electric vibrator until the concrete was close-grained. During the 28-day's curing, top concrete was stricken off with high-strength cement mortar to complement the shrinkage and another series of end plates was welded to seal the top ends of the specimens.

2.2. Material properties

According to the Chinese National standard (GB/T 228-2002), Metallic materials-tensile testing at ambient temperature, mechanical properties of the steel plate and reinforcement bars were tested. Carbon cold-rolled steel of Q190 grade (the characteristic value of yielding strength is 190 N/mm^2) and hot-rolled steel of Q235 grade (the characteristic value of yielding strength is 235 N/mm^2) were employed. The material properties are collected in Table 2.

Hot-rolled plane reinforcement of HPB235 grade (the characteristic value of yielding strength is 235 N/mm^2) and hot-rolled ribbed reinforcement of HRB335 grade (the characteristic value of yielding strength is 335 N/mm^2) were employed, for the bar stiffeners, hoops and the longitudinal reinforcements and of which details showed in Table 3.

The concrete denoted C30 and C40 (according to a concrete code in China GB50010-2002), with the mix proportion shown in Table 4, was poured into hollow tubes, along with prismatic standard test blocks with dimensions of 100 mm×100 mm×100 mm. Test specimens' curing lasted to the day of trial and the test cube blocks were tested to get the equivalent value of concrete compressive prismatic strength f_{ck}.

2.3. Experimental devices

The experiment was carried out at the Structural and Seismic Test Research Center, Harbin Institute of

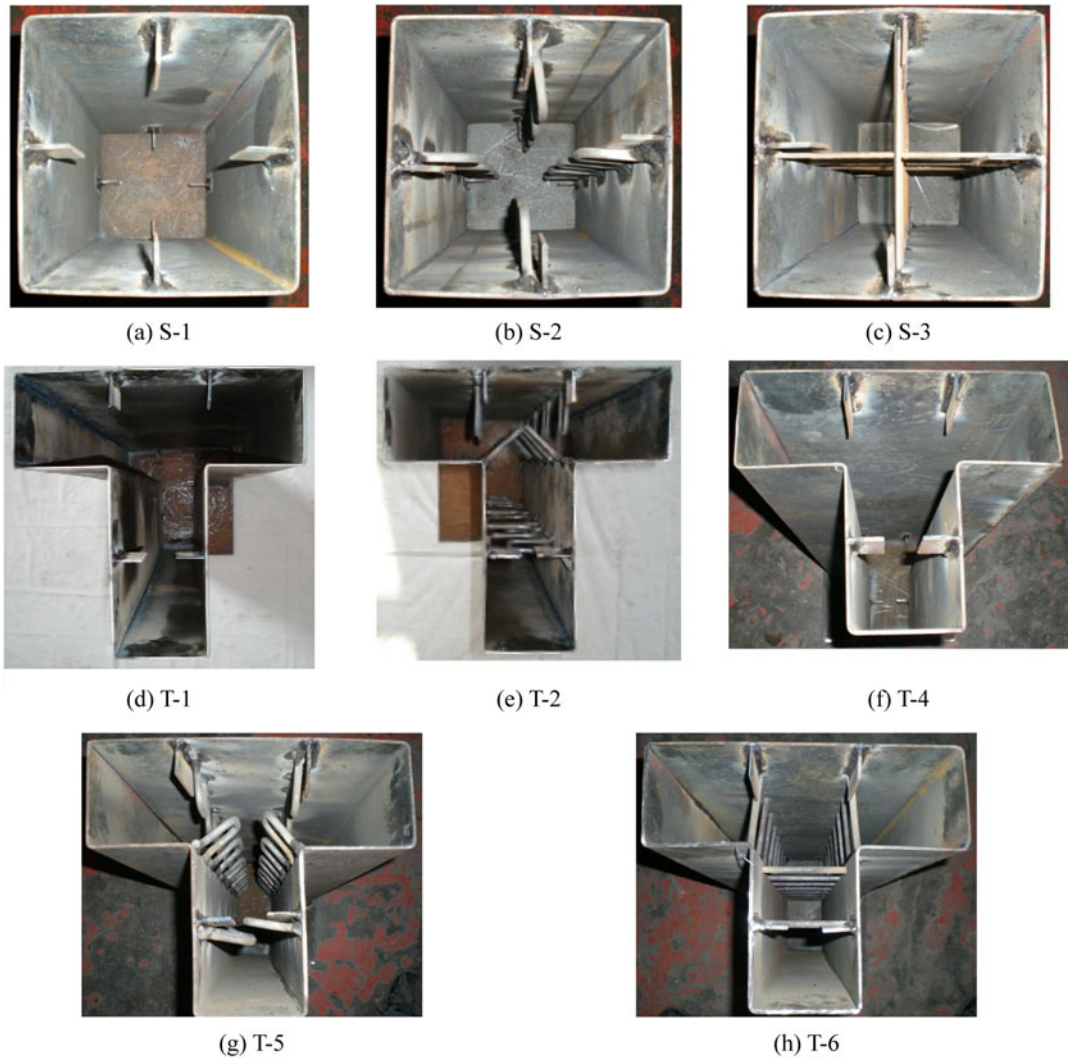

Figure 3. Cross sections of hollow steel tubes with stiffeners.

Technology. A 500t computer OSD hydraulic pressure press was used as loading device, with two articulated rigid plates to simulate fixed boundary conditions, in which the bottom rigid plate lifted the specimen and the top kept motionless. Two accessary columns, with adjustable length, were specially used to support the axial load along with the specimen, to stably get the load-displacement curves during descending stage, shown in Fig. 4.

The axial load was measured with a load sensor on the

Table 2. Material properties of the steel tubes

Specimen group	Steel grade	Thickness t (mm)	Yielding strength f_y (N/mm^2)	Ultimate strength f_u (N/mm^2)
I/III	Q235	3.49	315	434
II	Q190	2.00	162	283

Table 3. Material properties of the reinforcements

Specimen	Reinforcement	Grade	Diameter t_r (mm)	Yielding strength f_{yr} (N/mm^2)	Ultimate strength f_{ur} (N/mm^2)
T-2	Stiffener	HPB235	6.5	290	455
S-2/T-5/T-6	Stiffener	HPB235	8.0	304	463
T-3	Longitudinal reinforcement	HRB335	12.0	353	514
T-3	Hoop	HPB235	6.5	373	525

Table 4. Mix proportions of concrete (kg/m^3)

Group	Grade	Water	Portland cement	Sand	Gravel	Water reducing agent
I/III	C30	185	330	740	1030	8.6
II	C40	152	400	662	1178	4.0

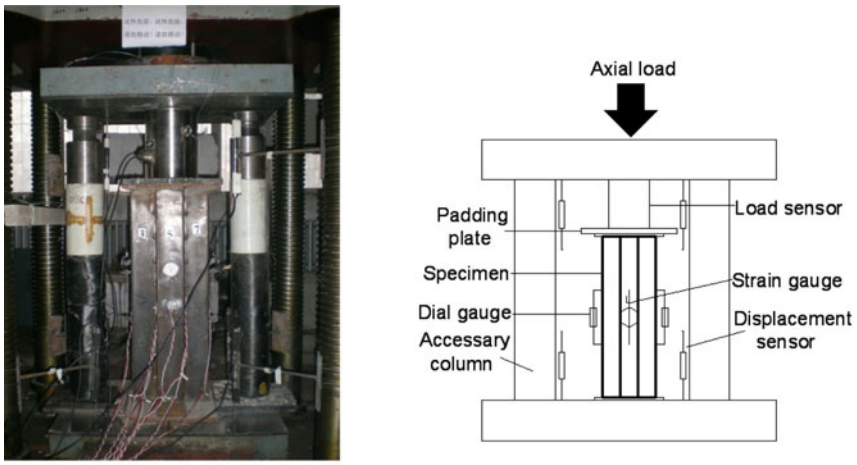

(a) Picture of loading (b) Illustrative drawing of loading

Figure 4. Loading devices.

top end plate of the specimen and a 20 mm-thick padding plate was sandwiched between them in order to get even axial loads, shown in Fig. 4.

Three independent methods were employed for axial displacement of the specimens: displacement sensors (LVDT) for overall axial displacement; dial gauges for displacement increment prior to local buckling; vertical strain gauges for local axial strain at the mid-height of four tube surfaces during elastic stage. Four displacement sensors (1, 2, 3 and 4) were placed at bottom and two (5 and 6 in parenthesis) were at top (in Fig. 5), so the effective displacement u_r after the specimen and devises were close-contact, is calculated with Eq. (1):

$$u_r=u_b-u_t \tag{1}$$

where u_b is the average data value of the bottom four sensors; u_t is the average data value of the top two sensors.

Four dial gauges were symmetrically arranged within 20 mm gage length at mid-height of each steel plate (in Fig. 5). Strain gauges (including vertical ones and transverse ones) were employed on the center of outer surfaces of tube (in Fig. 6), and specially, located at the point between two adjacent welds for the stiffened tube. The dial gauges and strain gauges were also used for the physical centering adjustment before actual loading.

The data from the load sensor and LVDTs were input into the Beijing spectrum instrument so that the axial load-displacement curves were real-time monitored.

2.4. Test phenomenon

During loading procedure, the material damage

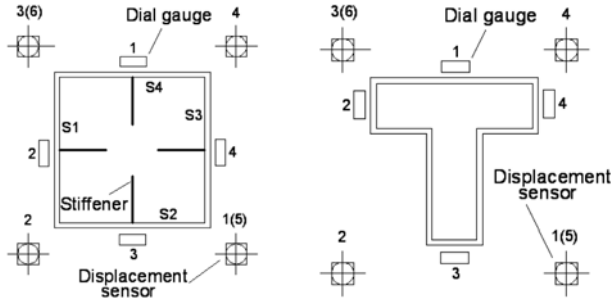

(a) square specimen (b) T-shaped specimen

Figure 5. Layout of dial gauges and displacement sensors.

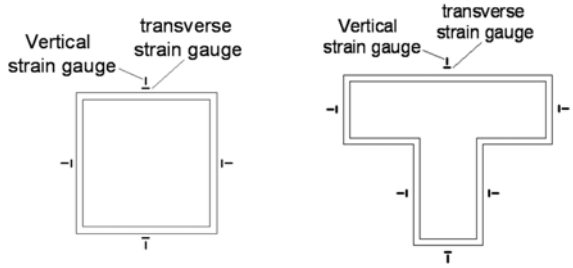

(a) Square specimen (b) T-shaped specimen

Figure 6. Layout of strain gauges for specimens.

gradually formed from the elasto-plastic stage to the completion of test. The macroscopic phenomenon was recorded to reasonably describe the specimen mechanical property, collaborated with the subsequent test data. To describe the test phenomenon conveniently, all the steel plate surfaces in cross sections are numbered (in Fig. 7).

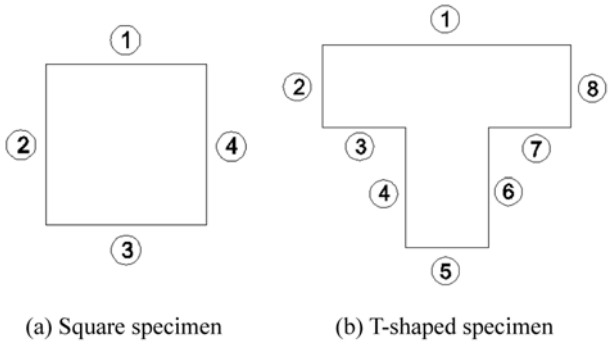

(a) Square specimen (b) T-shaped specimen

Figure 7. Surface numbering.

2.4.1. Concrete crushing and failure modes

In the loading process of the RC (T-3) specimen, several diagonal cracks firstly appeared in the web, followed by diagonal cracks at the intersection of flange and web. When approaching the peak load, transversal crushed cracks emerged gradually on all the surfaces, and the previous diagonal cracks developed into large longitudinal cracks. After loading, specimen's failure phenomenon was summarized as below: the crushed region was mainly located at the top half, and the concrete was seriously damaged, with the web more seriously than the flange. On the flange, long transversal cracks, along with several longitudinal cracks were located (shown in Fig. 8(a)), however without any concrete spalling. The diagonal cracks on the web developed to the surface 5 (Fig. 8(b)), and cause the top concrete of the surface crushed in large area, exposing the longitudinal bars and hoops. Cracks formed at the inner corners during loading, but without intensification (Fig. 8(c)).

For non-stiffened specimens (including square and T-shaped specimens), the confinement provided by tube was relatively weak, especially for T-1 specimen, which appeared to be in shear failure mode. Several diagonal cracks could be seen in the top and bottom, and small-area neighboring concrete was crushed to a little depth (shown in Fig. 9(b)), which revealed the concrete compressive strength wasn't fully used. These brittle fractural cracks were due to little confinement from steel tube after premature local buckling. Other non-stiffened specimens with smaller width-to-thickness ratio showed little concrete crush expansion (shown in Figs. 9(a), 9(c)), which was less than the steel tube buckling, so the separation (especially at the inner corner) between concrete and tube made them work individually and no complete exploration of material strength can be reached.

For stiffened specimens (including square and T-shaped specimens), concrete was damaged in local crushed mode, i.e. no obvious diagonal cracks but serious local trivial cracks. The crushed concrete located between two adjacent stiffener welds, while concrete at welds showed little damage (shown in Fig. 10), which indicates that stiffeners restrain the neighboring steel tube to provide confinement for concrete. The concrete was crushed more seriously than that without stiffeners, and rare separation between concrete and tube improve the exploration of material strength.

2.4.2. Steel buckling and stiffener behavior

The buckling occurrence was much later in the stiffened (both the battlement-shaped bar and the tensile bar/strip) specimens than in the non-stiffened specimens, and the out-of-plane deformation was greatly decreased. Due to the absence of stiffeners' hold, the steel tube of non-stiffened specimen buckled outward, separated from core concrete, presenting multi-wave buckling mode (shown in Fig. 9), especially for T-1 specimen. This adverse mechanism was noticeably improved by bar stiffeners in the stiffened specimens. The deformation at welds and inner corners was almost completely restrained so that the overall deformation was smaller (shown in Fig. 10).

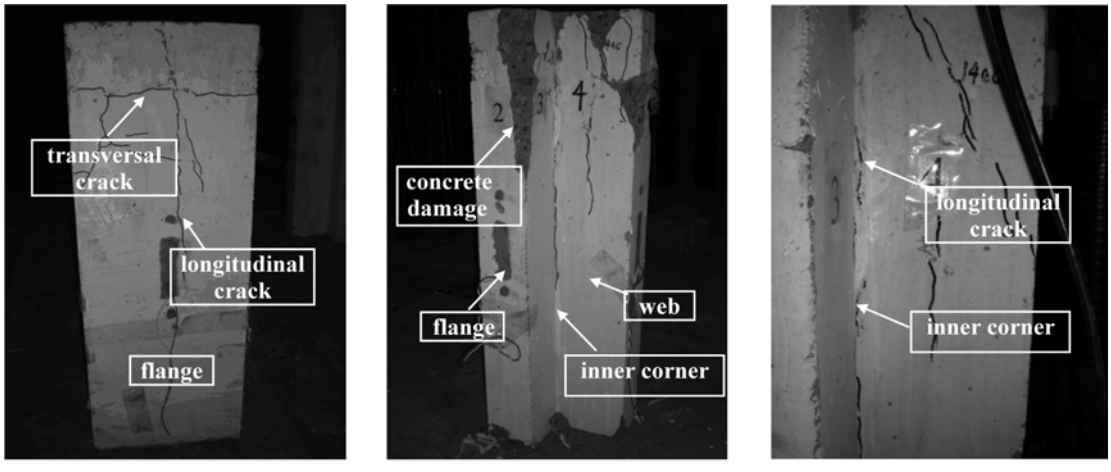

(a) (b) (c)

Figure 8. RC specimen (T-3).

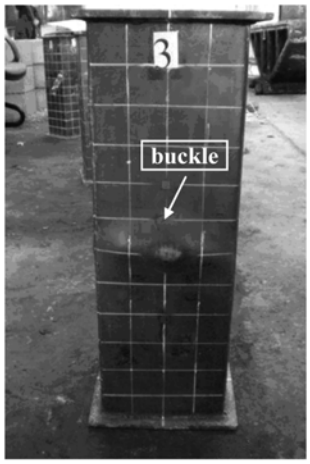

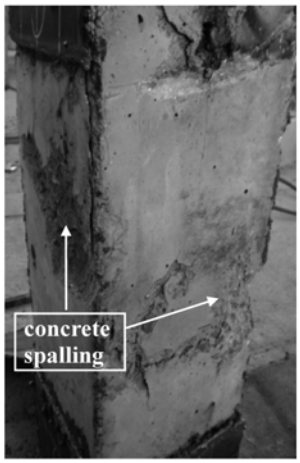

(a) Square specimen (S-1)

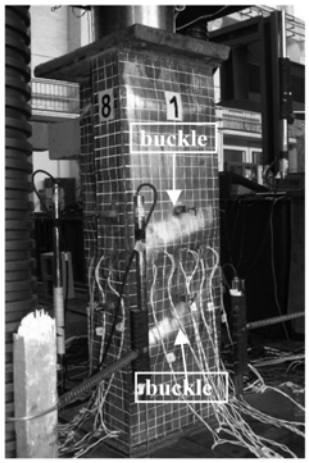

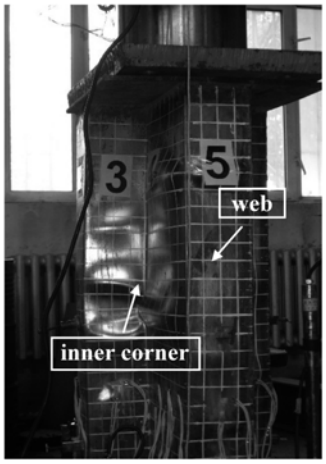

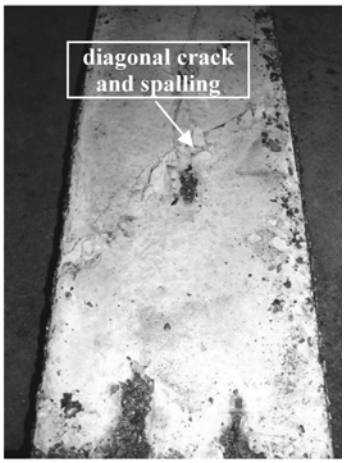

(b) T-shaped specimen (T-1)

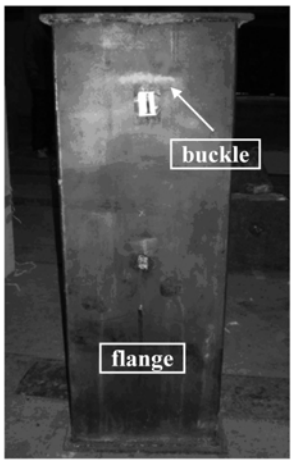

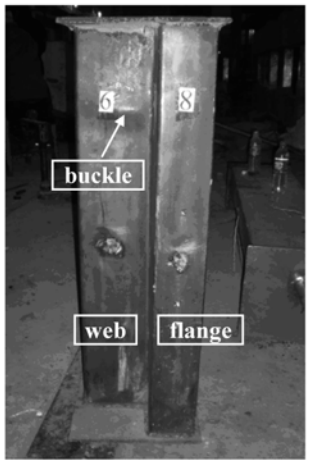

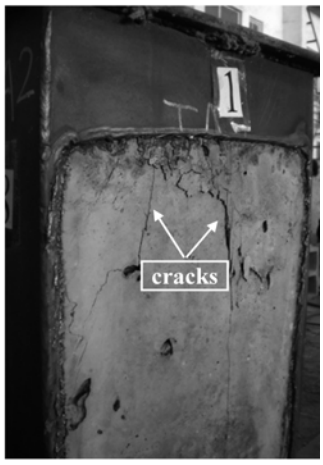

(c) T-shaped specimen (T-4)

Figure 9. Non-stiffened CFST specimens.

The battlement-shaped part vertical to tube effectively restrained the tube at welds to change its buckling modes. So the vertical part of bar stiffeners played more efficient influence than the parallel part on the buckling of steel tube. However, the embedment is not complete, due to the expansion of concrete. On the other side, the reaction of embedment to concrete by battlement-shaped bar is converted into tension strain harmful to concrete. The development of stiffener's advantages can be guaranteed only if it is fully fixed in the concrete. In the study, the

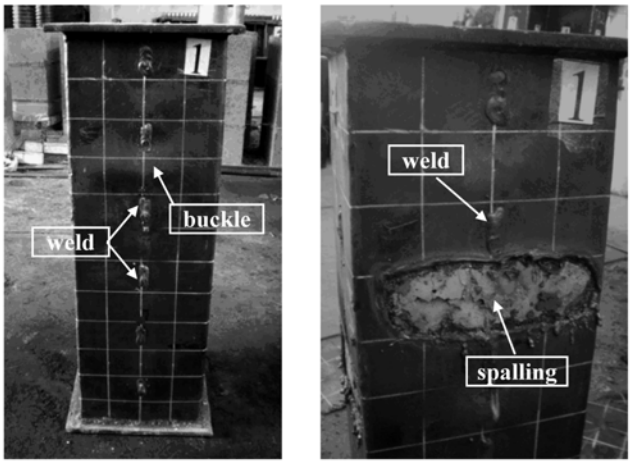

(a) Square specimen (S-3)

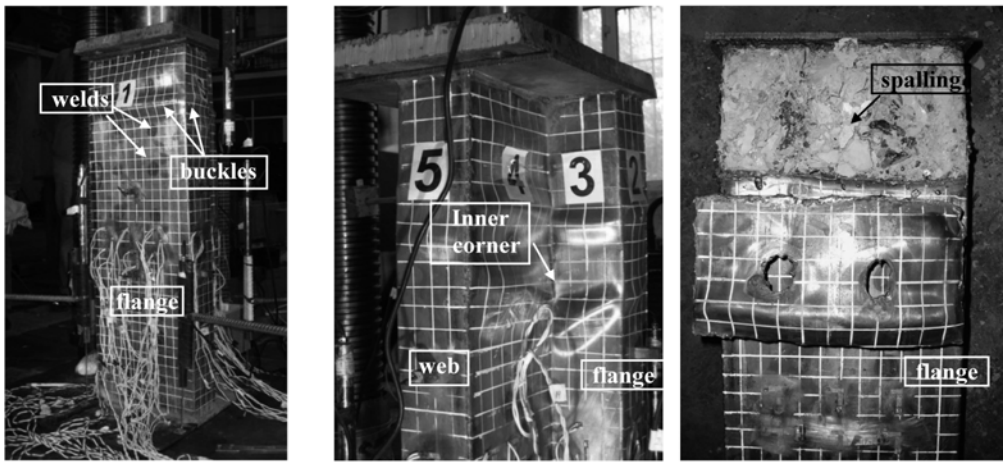

(b) T-shaped specimen (T-2)

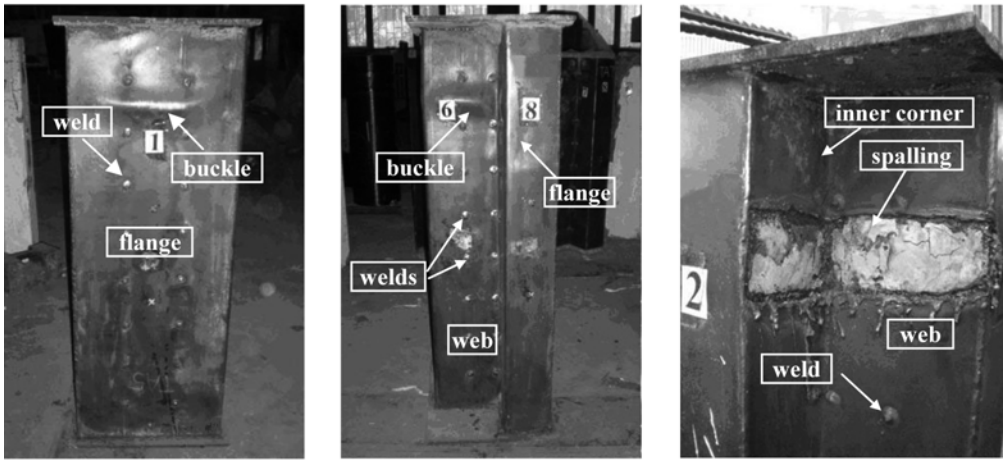

(c) T-shaped specimen (T-6)

Figure 10. Stiffened CFST specimens.

key factor is the embedment depth. Results from the experiment may reveal a reference value (larger than 50 mm) on the embedment depth for the battlement-shaped bar stiffeners, regarding the crushing depth of concrete. Restricted to narrow variation of parameters (such as cross-sectional dimension, concrete strength and steel tube thickness) in this paper, a comprehensive regulation of bar embedment depth considering parameters mentioned above needs further investigation.

The tensile bar is welded at two ends on the opposite

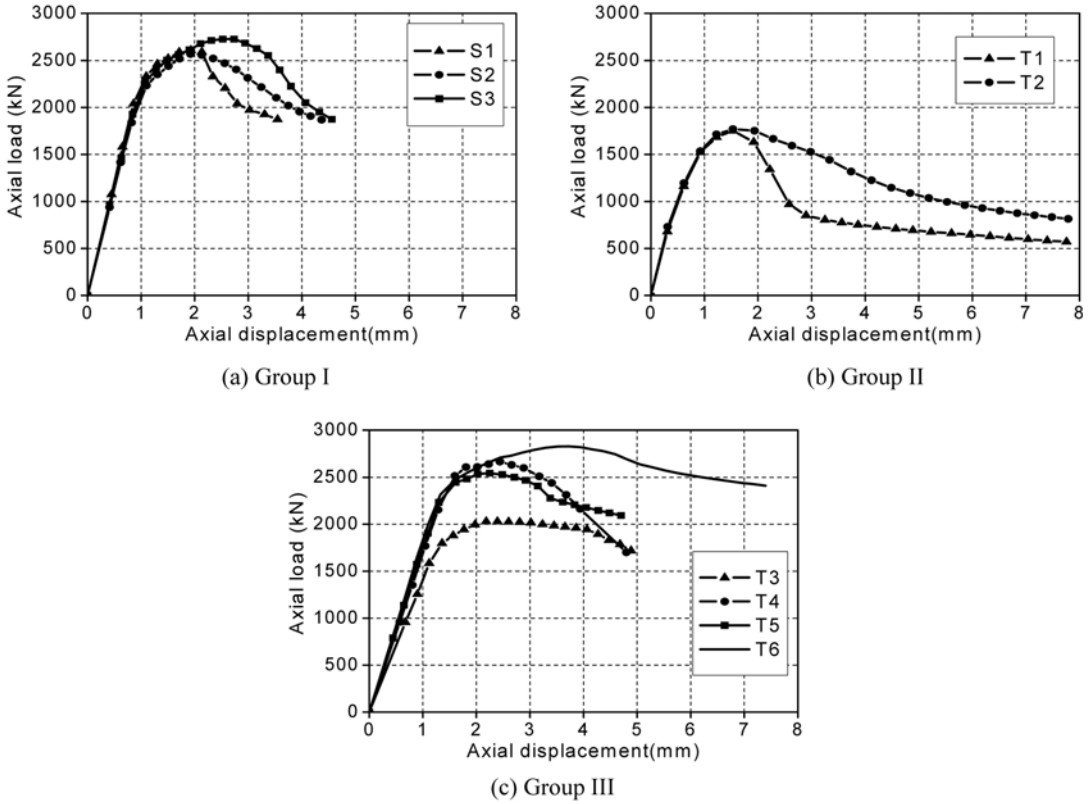

Figure 11. Axial load-displacement curves.

plates, taking full advantages of steel tensile property. In addition, the stiffener only interacts with steel tube, without any disadvantages on the concrete.

3. Analysis of Experimental Results

3.1. Axial load-displacement curves

Figure 11(a) shows the axial load-displacement relation curves of the square specimens (Group I). It is found that the ascending stiffness of the square CFST specimens is almost the same which indicates that the stiffeners have little effect at this stage. When approaching the peak resistance, behavioral differences are manifested in the curves. Especially for S-3 with tensile bar stiffeners, the resistance is higher than that of the non-stiffened and stiffened specimens with battlement-shaped bar stiffeners. The battlement-shaped bar stiffeners failed to increase the resistance of CFST stubs, and the reason may attribute to the defect caused by welding and the tensile stress in concrete brought by stiffeners' embedment. During the descending stage, the stiffeners played even more important role in enhancing mechanical behavior and the stiffened specimens give obviously better ductility than that of non-stiffened specimen. That was because the stiffeners effectively restrain the out-of-plane deformation of the tube and enhance the interaction of concrete and tube. Due to the tension property exploration and no adverse impact of tensile stress on the concrete, the specimen with tensile strip was provided with the best ductility.

Figure 11(b) shows the axial load-displacement curves of the Group II. It is found that the stiffened (T-2) and non-stiffened (T-1) T-shaped CFST possess similar ascending stiffness, yielding displacement, yielding resistance and peak resistance, but the former one takes advantage on the latter one in the ductility. During the early stage of loading, although the concrete expansion brought certain interaction between concrete and tube, the T-shaped tube, being similar or even worse than square tube, had no substantially high circumferential stress, and accordingly the confinement provided for concrete was relatively small, owing to the small tube thickness. The stiffeners played little role in mechanism enhancement before peak resistance. During the descending stage, with the axial displacement growing rapidly, the concrete expansion was substantially large, thus it was provided with relatively high confinement. The descending tendency is slowed down and the ductility of specimen is improved.

During the full loading procedure of Group III (in Fig. 11 (c)), the CFST specimens (especially the stiffened specimens) took advantages on the RC specimen, in the ascending stiffness, peak resistance and ductility. The failure modes and variation tendency of curves were similar with that in Group I and Group II. The stiffeners significantly improved the ductility of specimens, and specially, the tensile bar stiffeners effectively enhanced the peak resistance.

Table 5. Test results

Group	I			II		III			
Specimen	S-1	S-2	S-3	T-1	T-2	T-3	T-4	T-5	T-6
P_u (kN)	2630	2566	2766	1758	1788	2030	2672	2549	2827
P_n (kN)	2279	2279	2279	2055	2055	-	2477	2477	2477
SI	1.15	1.13	1.20	0.86	0.87	-	1.08	1.03	1.14
μ	1.97	2.59	2.75	2.07	3.07	3.06	2.19	2.66	4.22
DI	1.00	1.31	1.40	1.00	1.48	-	1.00	1.21	1.93

3.2. Mechanical performance index

Mechanical performance indexes are specifically calculated from the intuitional axial load-displacement curves and listed in the Table 5. The indexes and their variation tendency are described as followed:

The ultimate resistances P_u are increased in CFST specimens, especially in the stiffened specimens, compared with their nominal ultimate resistances P_n, except the group II, in which the steel tubes are insufficient for confinement, due to smaller thickness and lower tube strength. The definition of P_n is calculated by superimposing the resistances of individual steel and concrete with Eq. (2):

$$P_n=A_s f_y+A_c f_{ck} \tag{2}$$

where, f_y is the measured value of steel tube's yielding strength; f_{ck} is the equivalent value of concrete compressive prismatic strength deduced from measured compressive cube strength, according to the China national concrete standard, *Code for design of concrete structures* (GB50010-2002, 2002).

The ultimate test strength enhancement index (SI) reflects the positive interaction between concrete and steel tube, and can be described in Eq. (3). With the unfavorable inner corners, the SI of T-shaped specimens range from 1.03 to 1.14, smaller than that of square specimens from 1.13 to 1.20. The tensile bar stiffeners improve the SI of CFST, while the battlement-shaped bar stiffeners deteriorate it, owing to low confinement caused by tensile stress in concrete before descending stage.

$$SI=P_u/P_n \tag{3}$$

The ductility factors (μ) of the stiffened specimens are increased compared with that of the non-stiffened specimen. μ is defined as the ratio of axial strain corresponding to 85% ultimate test resistance during descending stage $\varepsilon_{0.85}$ to the yielding strain ε_y, in Eq. (4).

$$\mu=\varepsilon_{0.85}/\varepsilon_y \tag{4}$$

To investigate the enhancement of ductility by the stiffeners over that of the non-stiffened specimen, ductility enhancement index DI (listed in Table 5) is employed and defined in Eq. (5), where μ_0 is the ductility factor of the non-stiffened specimen. The stiffened CFST specimens (S-2, S-3, T-2, T-5 and T-6) are provided with higher increase in DI, especially for the specimens with tensile bar stiffeners (T-6).

$$DI=\mu/\mu_0 \tag{5}$$

3.3. Classification of the composite cross-section

The European Standard "Eurocode 4: Design of composite steel and concrete structures" (EN 1994-1-1, 2005) puts forward the classification of composite sections, which reflects the exploration level of material strength. To analyze the classification and material exploration of the composite sections in the experiment, the resistance at the first buckle P_b, the resistance at the steel tube yielding P_y, the ultimate resistance P_u, and the buckling resistance ratio BI (BI=P_b/P_y) are listed in Table 6, in which, if tube buckling occurs during the descending stage, the P_b takes the value of P_u.

It should be mentioned that the tube buckling is defined as the cross-sectional buckling appeared in the middle tube, where the buckling is only influenced by cross-sectional slenderness and concrete supporting, rather than end tube's buckling, which is caused by end concrete shrinkage and end tube's bearing load prior to concrete.

As listed in Table 6, the T-1 specimen buckled before reaching steel tube yielding, due to its flexible cross-sectional slenderness, which indicated the cross-section of T-1 belonged to the Class 4 grade in classification (EN 1994-1-1 2005). By adding stiffeners in T-2 specimen, the buckling loads was even over the yielding loads of the stiffened specimens, indicating that without thickening the tubes, the cross-section of the specimen was updated to the Class 3 grade, in which the stress in the extreme compression fiber of the steel components, assuming an elastic distribution of stresses, could reach the yield strength.

For the non-stiffened specimens as S-1 and T-4, tube buckling occurred after reaching yielding, and before peak resistance, which indicated the cross-section of S-1 and T-4 belonged to the Class 3 grade. By adding stiffeners in specimens S-2, S-3, T-5 and T-6, the buckling loads were closer to or even over the peak resistance of the stiffened specimens, that is to say, without thickening the tubes, the cross-sections of the specimens were updated to the Class 2 grade, in which the cross sections could develop their plastic resistance, but had limited displacement capacity because of local buckling.

The BI of S-1, S-2 and S-3 is much higher than that of

Table 6. Characteristic resistances of specimens

Group	I			II		III		
Specimen	S-1	S-2	S-3	T-1	T-2	T-4	T-5	T-6
P_b (kN)	2500	2566	2726	700	1175	2200	2549	2827
P_y (kN)	1065	1078	718	900	1000	1870	2545	2627
P_u (kN)	2630	2566	2726	1758	1788	2672	2549	2827
BI	2.35	2.38	3.80	0.78	1.18	1.18	1.01	1.08

T-4, T-5 and T-6, the reason of which may attribute to the different tube corner types, which are outer corners in the square tube, while outer and inner corners in the T-shaped tube. The concrete could only restrain the inward deformation of tube, but failed to restrain its outward deformation. Therefore, the concrete and steel tube separated from each other at the inner corners, weakening the boundary conditions of adjacent plates and deteriorating the buckling resistance of specimens.

The use of battlement-shaped bar or tensile bar/strip may make the geometry of the cross-section a little more complex, compared with the non-stiffened specimen. However, the improvement in the mechanical properties of square and T-shaped CFST by these stiffeners is obvious. Besides, the welding work of these new stiffeners is much less than that of traditional rib stiffeners, inducing slight unfavorable influence on the steel tubes. With the maturity of manufactory production, the batch fabrication and welding of stiffeners can save the manpower and bring comprehensive economic benefits.

4. Conclusions

The battlement-shaped bar and tensile bar stiffeners are first put forward in this paper, to improve the axial compressive behavior of the square and T-shaped CFST specimens. Experimental study of 9 stubs in three groups subjected to axial loads was conducted. Results reveal that: the CFST columns takes advantage on the RC specimen in the ascending stiffness, peak resistance. By restraining the out-of-plane deformation at welds, the battlement-shaped bar and tensile bar/strip postpone the tube buckling, and accordingly improve the confinement for concrete and ductility of specimens. Compared with the columns with battlement-shaped bar, those stiffened with tensile bar/strip present higher compressive resistance and the fabrication is more practicable.

The classification of composite sections can be upgraded by stiffeners, and the steel strength exploration is significantly raised. By adding stiffeners and without thickening the tubes, for specimens with small tube thickness in Group II, the buckling loads are closer to or even over the yielding loads. Similarly for specimens with large tube thickness in Group I and III, the buckling loads are closer to or even over the peak resistances.

Acknowledgments

The work described in this paper was jointly funded by the National Natural Science Foundation of China under Grant No. 50708028, Scientific Research Foundation of Harbin Institute of Technology under Grant No. HIT.2003.43, and National Key Technology R&D Program during the 11th Five-Year Plan Period of China under Grant No. 2006BAJ01B02.

References

Cai, J. and He, Z. Q. (2005). "Axial load behavior of square CFT stub column with binding bars." *Journal of Constructional Steel Research*, 62, pp. 472-483.

Chen, Z. Y. (2003). *Construction techniques of concrete-filled rectangular steel tube (CFRT) columns and axial bearing capacity of concrete-filled special-shaped steel tube stubs.* Dissertation for the Master's Degree in Engineering, Tongji Univercity (in Chinese).

Cheng, T. and Thomas, H. (1989). "T-shaped reinforced concrete members under biaxial bending and axial compression." *ACI Structural Journal*, 86(4), pp. 2576-2595.

Dundar, C. and Sahin, B. (1993). "Arbitrarily shaped reinforced concrete members subjected to biaxial bending and axial load." *Computers & Structures*, 49(4), pp. 643-662.

Gao, D. X., Ke, J., and Wang, L. H. (2005). "Seismic behavior analysis of special-shaped column frame structure." *Journal of Xi'an University of Technology*, 21(3), pp. 285-288 (in Chinese).

Joaquin, M. (1979). "Design aids for L-shaped reinforced concrete columns." *ACI Structural Journal*, 76(49), pp. 1197-1216.

Mallikarjuna and Mahadevappa, P. (1992). "Computer aided analysis of reinforced concrete columns subjected to axial compression and bending — I L-shaped sections." *Computers & Structures*, 44(5), pp. 1121-1138.

Tao, Z., Han, L. H., and Wang, Z. B. (2005). "Experimental behaviors of stiffened concrete-filled thin-walled hollow steel structural (HSS) stub columns." *Journal of Constructional Steel Research*, 61, pp. 962-983.

Wang, D. and Lv, X. L. (2005). "Experimental study on seismic behavior of concrete-filled steel T-section and L-section columns." *Journal of Building Structures*, 26(4), pp. 39-44, 106 (in Chinese).

Wang, T. C., Li, X. H., Wang, T. Z., and Kang, G. Y. (2007). "Hysteretic behavior of frame with specially shaped columns subjected to cyclic loading." *Journal of Jilin University, Engineering and Technology Edition*, 37(1), pp. 224-228 (in Chinese).

Wang, Y. Y., Yang, Y. L., Zhang, S. M., and Liu, J. P. (2009). "Seismic behaviors of concrete-filled T-shaped steel tube columns." *Key Engineering Materials*, 400-402, pp. 667-683.

Yau, C. Y., Chan, S. L., and So, A. K. W. (1993). "Biaxial bending design of arbitrarily shaped reinforced concrete column." *ACI Structural Journal*, 90(3), pp. 269-279.

Zhang, D. and Ye, X. G. (2003). "Non-linear analysis of special-shaped reinforced concrete columns." *Journal of Hefei University of Technology*, 26(4), pp. 490-494 (in Chinese).